Journal of Applied Mathematics and Physics, 2016, 4, 1600-1609
Published Online August 2016 in SciRes. http://www.scirp.org/journal/jamp
http://dx.doi.org/10.4236/jamp.2016.48170

Spline Solution for the Nonlinear Schrödinger Equation

Bin Lin

School of Mathematics and Computation Science, Lingnan Normal University, Zhanjiang, China
Email: linbin167@163.com

Received 13 July 2016; accepted 22 August 2016; published 25 August 2016

Abstract

We develop an exponential spline interpolation method to solve the nonlinear Schrödinger equation. The truncation error and stability analysis of the method are investigated and the method is shown to be unconditionally stable. The conservation quantities are computed to determine the conservation properties of the problem. We will describe the method and present numerical tests by two problems. The numerical simulations results demonstrate the well performance of the proposed method.

Keywords

Nonlinear Schrödinger Equation, Exponential Spline Interpolation, Gross-Pitaevskii Equation, Mass and Energy Conservation

1. Introduction

Consider the following nonlinear Schrödinger equation

$$mu_t + \lambda_1 u_{xx} + \lambda_2 |u|^2 u + \varepsilon(x,t)u = 0, \tag{1}$$

With the boundary conditions

$$u(c,t) = \beta_1(t), u(d,t) = \beta_2(t), t \geq 0 \tag{2}$$

And the initial condition

$$u(x,0) = u^0(x), x \in \mathbb{R}, \tag{3}$$

where $m = \sqrt{-1}$, $u(x,t)$ is the complex-valued wave function. λ_1 and λ_2 are constant, $\varepsilon(x,t)$ is a

How to cite this paper: Lin, B. (2016) Spline Solution for the Nonlinear Schrödinger Equation. *Journal of Applied Mathematics and Physics*, **4**, 1600-1609. http://dx.doi.org/10.4236/jamp.2016.48170

bounded real function. This equation plays important roles in nonlinear physics. It can describe many nonlinear phenomena including plasma physics [1], hydrodynamics [1] [2], self-focusing in laser pulses [3], propagation of heat pulses in crystals, models of protein dynamics [4], quantum mechanics [5], models of energy transfer in molecular systems [6] and quantum mechanics and optical communication [7]-[9] and so on.

In the past few years a great deal of efforts has been expended to solve NLS equations. It is more difficult to find the analytical solutions of the NLS equation, so the study of the numerical solution of NLS equation in the theory and application is important. Its numerical solutions have been researched by many authors. For example, finite difference method [10] [11], quasi-interpolation scheme [12], quadratic B-spline finite element scheme [13], compact split-step finite difference method and pseudo-spectral collocation method [14] [15], exponential spline method [16], spline methods [17] [18], split-step orthogonal spline collocation method [19], a high-order and accurate method [20], linearly implicit conservative scheme [21].

The aim of this paper is to give an exponential spline interpolation method for the NLS equation. The paper is organized as follows. In Section 2, construction of the method is presented. The stability analysis of the scheme is investigated in Section 3. In Section 4, the computation of conserved quantities and error norms are given. In Section 5, two numerical examples are presented to demonstrate our theoretical results. The last section is a brief conclusion.

2. Construction of Exponential Spline Interpolation Method

We set up a grid in the x,t plane with grid points $\left(x_i,t_j\right)$ and uniform grid spacing h and k, where $x_i = a + ih, h_{i+1} = x_{i+1} - x_i, i = 0,1,2,\cdots,N$ and $t_j = jk, j = 0,1,2,\cdots$.

In the interval $\left[x_i, x_{i+1}\right]$, a exponential spline function $S_i\left(x,t_j\right)$ is given by

$$S_i\left(x,t_j\right) = c_{1i}^j + c_{2i}^j\left(x - x_i\right) + c_{3i}^j\psi_i\left(x - x_i\right) + c_{4i}^j\phi_i\left(x - x_i\right), \tag{4}$$

where $c_{1i}, c_{2i}, c_{3i}, c_{4i}$ are coefficients to be determined, ψ_i and ϕ_i are the auxiliary functions which contain a stiffness parameter p_{i+1} which will be used to raise the accuracy of the method, on the support $\left[x_i, x_{i+1}\right]$ and are given by

$$\psi_i\left(x\right) = 2\left[\cosh\left(p_{i+1}\left(x - x_i\right)\right) - 1\right] \Big/ p_{i+1}^2, \tag{5}$$

$$\phi_i\left(x\right) = 6\left[\sinh\left(p_{i+1}\left(x - x_i\right)\right) - p_{i+1}\left(x - x_i\right)\right] \Big/ p_{i+1}^2, \tag{6}$$

Since the Taylor series expansions of the hyperbolic functions are

$$\sinh\left(px\right) = px + \frac{\left(px\right)^3}{3!} + \frac{\left(px\right)^5}{5!} + \cdots, \tag{7}$$

$$\cosh\left(px\right) = 1 + \frac{\left(px\right)^2}{2!} + \frac{\left(px\right)^4}{4!} + \cdots, \tag{8}$$

We note that ψ_i and ϕ_i tend to $\left(x - x_i\right)^2$ and $\left(x - x_i\right)^3$ in the limit of p tending to zero, and in the opposite limit of p tending to infinity the nonlinear terms in ψ_i and ϕ_i vanish as $1/p$.

So the exponential spline defined above share a number of interesting properties:

(1) When $p \to 0$, $S_i\left(x,t_j\right)$ reduces to cubic spline; when $p \to \infty$, $S_i\left(x,t_j\right)$ reduces to linear spline.

(2) A change of character of the exponential spline function is from linear to third order polynomial on adjacent support intervals.

(3) In the general case the stiffness parameters p are different on every interval which provides the extremely high flexibility of the exponential spline function.

We wish to find c_{ni}^j in Equation (4), $n = 1,2,3,4$, Letting $M_i^j = S_\Delta^{(2)}\left(x,t_j\right)$ be the unknown second derivative of the exponential spline of interpolation at the grid points, we can obtain the following representation for $S_\Delta\left(x,t_j\right)$ on $\left[x_i, x_{i+1}\right]$ in terms of the known interpolation data u_i^j, u_{i+1}^j and the unknown spline second derivatives M_i^j, M_{i+1}^j

$$S_\Delta(x,t_j)=\frac{x-x_{i+1}}{x_i-x_{i+1}}u_i^j+\frac{x-x_i}{x_{i+1}-x_i}u_{i+1}^j-\frac{M_i^j}{p_{i+1}^2}\left[\frac{\sinh(p_{i+1}(x-x_{i+1}))}{\sinh(p_{i+1}(x_i-x_{i+1}))}-\frac{x-x_{i+1}}{x_i-x_{i+1}}\right]$$
$$+\frac{M_{i+1}^j}{p_{i+1}^2}\left[\frac{\sinh(p_{i+1}(x-x_i))}{\sinh(p_{i+1}(x_{i+1}-x_i))}-\frac{x-x_i}{x_{i+1}-x_i}\right],x\in[x_i,x_{i+1}], \tag{9}$$

The terms involving the values u_i^j and u_{i+1}^j represent the linear interpolation part of $S_\Delta(x,t_j)$. The terms involving the second derivatives M_i^j and M_{i+1}^j introduce the curvature.

The function $S_\Delta(x,t_j)$ on the interval $[x_{i-1},x_i]$ is obtained with $i-1$ replacing *i* in Equation (9).

The continuity requirement for the first derivative $S_\Delta^{(1)}(x,t_j)$ at the point x_i yields the following equation:

$$A_iM_{i-1}^j+(B_i+B_{i+1})M_i^j+A_{i+1}M_{i+1}^j=\frac{u_{i+1}^j-u_i^j}{h_{i+1}}-\frac{u_i^j-u_{i-1}^j}{h_i}, \tag{10}$$

where $A_i=h_i\frac{\sinh(p_ih_i)-p_ih_i}{p_i^2\sinh(p_ih_i)},B_i=h_i\frac{p_ih_i\cosh(p_ih_i)-\sinh(p_ih_i)}{p_i^2\sinh(p_ih_i)}$,

Remark 1.

(1) By expanding Equation (10) in Taylor series, the truncation error for Equation (10) is of the form

$$\begin{aligned}T_i^j&=\frac{u_{i+1}^j-u_i^j}{h_{i+1}}-\frac{u_i^j-u_{i-1}^j}{h_i}-A_iD_x^2u_{i-1}^j-(B_i+B_{i+1})D_x^2u_i^j-A_{i+1}D_x^2u_{i+1}^j\\&=\left[\frac{h_i}{2}(\sigma_i+1)-A_i-A_{i+1}-B_i-B_{i+1}\right](u_{2x})_i^j+\left[\frac{h_i}{6}(\sigma_i^2-1)+A_i-A_{i+1}\sigma_i\right]h_i(u_{3x})_i^j\\&\quad+\left[\frac{h_i}{12}(\sigma_i^3+1)-A_i-A_{i+1}\sigma_i^2\right]\frac{h_i^2}{2}(u_{4x})_i^j+\left[\frac{h_i}{20}(\sigma_i^4-1)+A_i-A_{i+1}\sigma_i^3\right]\frac{h_i^3}{6}(u_{5x})_i^j\\&\quad+\left[\frac{h_i}{30}(\sigma_i^5+1)-A_i-A_{i+1}\sigma_i^4\right]\frac{h_i^4}{24}(u_{6x})_i^j+O(h_i^5),\end{aligned} \tag{11}$$

where $\sigma_i=h_{i+1}/h_i,h_{i+1}=x_{i+1}-x_i$.

For $A_i=\frac{h}{12}(-\sigma_i^2+\sigma_i+1),A_{i+1}=\frac{h}{12\sigma_i}(\sigma_i^2+\sigma_i-1)$, $B_i+B_{i+1}=\frac{h_i}{12\sigma_i}(\sigma_i^3+4\sigma_i^2+4\sigma_i+1)$, the truncation error in space of the relation (10) is of $O(h^4)$.

From Equation (10), we can obtain

$$A_iM_{i-1}^j+(B_i+B_{i+1})M_i^j+A_{i+1}M_{i+1}^j=\frac{\sigma_iu_{i-1}^j-(\sigma_i+1)u_i^j+u_{i+1}^j}{\sigma_ih_i}, \tag{12}$$

Or

$$A_iM_{i-1}^{j+\frac{1}{2}}+(B_i+B_{i+1})M_i^{j+\frac{1}{2}}+A_{i+1}M_{i+1}^{j+\frac{1}{2}}=\frac{\sigma_iu_{i-1}^{j+\frac{1}{2}}-(\sigma_i+1)u_i^{j+\frac{1}{2}}+u_{i+1}^{j+\frac{1}{2}}}{\sigma_ih_i}, \tag{13}$$

Further, when $\sigma_i=1$, then $h=h_i=h_{i+1}$, $A_i=A_{i+1}=\frac{h}{12},B_i+B_{i+1}=\frac{10h}{12}$, the truncation error in space of the relation (10) is of $O(h^5)$, Equation (2.7) can be rewritten as

$$M_{i+1}^j+10M_i^j+M_{i-1}^j=\frac{12}{h^2}\left(u_{i+1}^j-2u_i^j+u_{i-1}^j\right), \tag{14}$$

$$M_{i+1}^{j+\frac{1}{2}}+10M_i^{j+\frac{1}{2}}+M_{i-1}^{j+\frac{1}{2}}=\frac{12}{h^2}\left(u_{i+1}^{j+\frac{1}{2}}-2u_i^{j+\frac{1}{2}}+u_{i-1}^{j+\frac{1}{2}}\right), \tag{15}$$

In order to get the error estimates of Equation (10), we put $E=\mathrm{e}^{hD}$ in Equation (12), where *E* and *D* are the shift and differential operators respectively, and expand them in powers of hD, we have

$$M_i^j = \frac{12}{h^2}\frac{E-2I+E^{-1}}{E+10I+E^{-1}}u_i^j = u_{xx}\left(x_i,t_j\right)+O\left(h^4\right), i=1,2,\cdots,N. \tag{16}$$

Or

$$\left(u_{xx}\right)_i^j = M_i^j + O\left(h^4\right), i=1,2,\cdots,N. \tag{17}$$

At the grid point $\left(x_i,t_j\right)$, Equation (1) can be discretized by

$$m\frac{u_i^{j+1}-u_i^j}{k}+\lambda_1\left(u_{xx}\right)_i^{j+\frac{1}{2}}+\varepsilon_i^{j+\frac{1}{2}}u_i^{j+\frac{1}{2}}+\lambda_2\frac{\left|u_i^{j+1}\right|^2+\left|u_i^j\right|^2}{2}u_i^{j+\frac{1}{2}}+O\left(k^2\right)=0, \tag{18}$$

From Equation (18), we have

$$M_{i-1}^{j+\frac{1}{2}} = -m\frac{u_{i-1}^{j+1}-u_{i-1}^j}{k\lambda_1}-\frac{1}{\lambda_1}\left(\varepsilon_{i-1}^{j+\frac{1}{2}}+\lambda_2\frac{\left|u_{i-1}^{j+1}\right|^2+\left|u_{i-1}^j\right|^2}{2}\right)u_{i-1}^{j+\frac{1}{2}}+O\left(k^2\right), \tag{19}$$

$$M_{i}^{j+\frac{1}{2}} = -m\frac{u_{i}^{j+1}-u_{i}^j}{k\lambda_1}-\frac{1}{\lambda_1}\left(\varepsilon_{i}^{j+\frac{1}{2}}+\lambda_2\frac{\left|u_{i}^{j+1}\right|^2+\left|u_{i}^j\right|^2}{2}\right)u_{i}^{j+\frac{1}{2}}+O\left(k^2\right), \tag{20}$$

$$M_{i+1}^{j+\frac{1}{2}} = -m\frac{u_{i+1}^{j+1}-u_{i+1}^j}{k\lambda_1}-\frac{1}{\lambda_1}\left(\varepsilon_{i+1}^{j+\frac{1}{2}}+\lambda_2\frac{\left|u_{i+1}^{j+1}\right|^2+\left|u_{i+1}^j\right|^2}{2}\right)u_{i+1}^{j+\frac{1}{2}}+O\left(k^2\right), \tag{21}$$

Substituting Equation (19), Equation (20) and Equation (21) into Equation (15) and after some simplifications, we obtain

$$F_{1i}u_{i-1}^{j+1}+F_{2i}u_i^{j+1}+F_{3i}u_{i+1}^{j+1}=F_{1i}^*u_{i-1}^j+F_{2i}^*u_i^j+F_{3i}^*u_{i+1}^j \tag{22}$$

where $i=1,2,\cdots,N,\ j=1,2,\cdots,\delta_i^j=\varepsilon_i^{j+\frac{1}{2}}+\lambda_2\frac{\left|u_i^{j+1}\right|^2+\left|u_i^j\right|^2}{2}$,

$$F_{1i}=\frac{A_i}{\lambda_1}\left(2m/k+\delta_{i-1}^j\right)+\frac{1}{h^2}, F_{2i}=\frac{B_i+B_{i+1}}{\lambda_1}\left(2m/k+\delta_i^j\right)-\frac{\sigma_i+1}{\sigma_i h_i},$$

$$F_{3i}=\frac{A_{i+1}}{\lambda_1}\left(2m/k+\delta_{i+1}^j\right)+\frac{1}{\sigma_i h_i}, F_{1i}^*=\frac{A_i}{\lambda_1}\left(-2m/k+\delta_{i-1}^j\right)+\frac{12}{h^2},$$

$$F_{2i}^*=\frac{B_i+B_{i+1}}{\lambda_1}\left(-2m/k+\delta_i^j\right)-\frac{24}{h^2}, F_{3i}^*=\frac{A_i}{\lambda_1}\left(-2m/k+\delta_{i+1}^j\right)+\frac{12}{h^2}.$$

The local truncation error of the relation (22) is of $O\left(k^2+h^4\right)$.

The boundary conditions (2) and the system given in the Equation (22) consists of $N+2$ equations in $N+2$ unknown. We can write this system in a matrix form as follows:

$$FU^{j+1}=F^*U^j, \tag{23}$$

where $U^j=\left(u_0^j,u_1^j,\cdots,u_N^j,u_{N+1}^j\right)^{\mathrm{T}}$,

Once the vectors U^0 are computed, $U^n, n=1,2,3,\cdots$, unknown vectors can be found repeatedly by solving the recurrence relation (23).

3. Stability Analysis

Following the von Neumann technique, we first linearize the nonlinear term in Equation (18) by making the quantity δ_i^j as locally constant δ and assume that the numerical solution can be expressed by means of a

Fourier series

$$u_i^j = \eta^j \exp(m\varphi ih) \tag{24}$$

where $m = \sqrt{-1}$, η^j is the amplitude at time level *j*, φ is the wave number and *h* is the element size. Substituting Equation (24) into Equation (22), the amplification factor can be written as

$$\eta = \frac{F_{1i}^* e^{-m\varphi h} + F_{2i}^* + F_{3i}^* e^{m\varphi h}}{F_{1i} e^{-m\varphi h} + F_{2i} + F_{3i} e^{m\varphi h}} \tag{25}$$

Using Eulers formula, we have

$$\eta = \frac{X_1 + mY_1}{X_2 + mY_2},$$

where $X_1 = X_2 = \left(\frac{\delta}{\lambda_1} + \frac{12}{h^2}\right)\cos(\varphi h) + \frac{10\delta}{\lambda_1} - \frac{24}{h^2}, Y_2 = -Y_1 = \frac{4}{k\lambda_1}\cos(\varphi h) + \frac{40}{k\lambda_1}$,

Since

$$|\eta| = \sqrt{\frac{X_1^2 + Y_1^2}{X_2^2 + Y_2^2}} = 1,$$

Thus this method is unconditionally stable.

4. Computation of Conserved Quantities and Error Norms

The nonlinear Schrödinger equation possesses two conservation quantities:

(1) Mass conservation:

$$C_1^{exact} = \int_a^b |u(x,t)|^2 \, dx, \tag{26}$$

Calculated by

$$C_1 = h\sum_{j=0}^{N} |u_j^n|^2, \tag{27}$$

(2) Energy conservation: If $\lambda_1(t)$ and $\lambda_2(t)$ are independent of *t*, then

$$C_2^{exact} = \int_a^b \left(\lambda_1 |u_x(x,t)|^2 - \varepsilon(x)|u(x,t)|^2 - \frac{\lambda_2}{2}|u(x,t)|^4\right) dx, \tag{28}$$

Calculated by

$$C_2 = h\sum_{j=0}^{N}\left[\lambda_1 \left|(u_x)_j^n\right|^2 - \varepsilon_i |u_j^n|^2 - \frac{\lambda_2}{2}|u_j^n|^4\right], \tag{29}$$

where u_j^n and *u* are the approximate solution at *n*-th time step at *j*-th node and exact solution, respectively.

The maximum error norm L_∞ and discrete root mean square error norm L_2 will be calculated

$$L_\infty(h,k) = \|u - u^n\|_\infty = \max_{0\le i\le N} |u(x_i) - u_i^n| \tag{30}$$

$$L_2(h,k) = \|u - u^n\|_2 = \sqrt{h\sum_{i=0}^{N} |u(x_i) - u_i^n|^2} \tag{31}$$

The relative error of numerical solution is defined as

$$E^r = \frac{\sqrt{\sum_{i=1}^{N} |u(x_i) - u_i^n|^2}}{\sqrt{\sum_{i=1}^{N} |u_i^n|^2}} \tag{32}$$

5. Numerical Results

In the section, we present the results of our numerical experiments for the proposed scheme described in the previous section.

Example 1. Consider the one dimensional Gross-Pitaevskii equation

$$mu_t + \frac{1}{2}u_{xx} - \cos^2(x)u - |u|^2 u = 0, x \in [0, 2\pi], t \geq 0 \tag{33}$$

With the analytical solution

$$u(x,t) = \mathrm{e}^{-m\frac{3t}{2}} \sin(x), \tag{34}$$

Conserved quantities and error norms at various times are recorded in **Table 1**. The real and imaginary parts of the numerical and exact solutions are tabulated in **Table 2**, the numerical results reveal the accuracy of the proposed method.

The absolute error at different space step sizes *h* at time $t = 1$ are shown in **Figure 1**, it can be seen that the absolute errors becomes smaller as decreasing *h*.

Example 2. Consider the equation (1) with $\lambda_1 = -1, \lambda_2 = 1,$

$$\varepsilon(x,t) = 4(x-2t)^2 - \mathrm{e}^{-2(x-2t)^2}, \tag{35}$$

The exact solution of this problem is

$$u(x,t) = \mathrm{e}^{-(x-2t)^2 + m(-x+3t)}, \tag{36}$$

Table 1. Conserved quantities and error norms at various times for example 1 with $k = 0.01, h = \frac{2\pi}{64}, a = 0, b = 2\pi$.

t	C_1	C_2	L_∞	L_2	E^r
5.0	3.14159265358952	5.00720563249462	1.4158e−004	2.5096e−004	1.4158e−004
10	3.14159265358946	5.00720563249418	2.8317e−004	5.0191e−004	2.8317e−004
20	3.14159265358965	5.00720563249524	5.6635e−004	1.0038e−003	5.6635e−004
30	3.14159265358984	5.00720563234957	8.4953e−004	1.5057e−003	8.4953e−004

$C_1^{0exact} = C_1^0 = 3.14159265358979$

Table 2. The real and imaginary parts of the numerical and exact solutions for Example 1 with $k = 0.001, h = \frac{2\pi}{64},$. $a = 0, b = 2\pi, t = 1$.

x_i	Real parts			Imaginary parts		
	Exact solution	Approximation	Absolute error	Exact solution	Approximation	Absolute error
$\frac{\pi}{4}$	0.05001875498139	0.05001908991577	3.35e-007	−0.70533546922731	−0.70533544547538	2.37e−008
$\frac{\pi}{2}$	0.07073720166770	0.07073767533643	4.73e-007	−0.99749498660405	−0.99749495301379	3.35e−008
$\frac{3\pi}{4}$	0.05001875498139	0.05001908991578	3.35e-007	−0.70533546922731	−0.70533544547537	2.37e−008
$\frac{5\pi}{4}$	−0.05001875498139	−0.05001908991578	3.35e-007	0.70533546922731	0.70533544547538	2.37e−008
$\frac{6\pi}{4}$	−0.07073720166770	−0.07073767533646	4.73e-007	0.99749498660405	0.99749495301376	3.36e−008
$\frac{7\pi}{4}$	−0.05001875498139	−0.05001908991577	3.35e-007	0.70533546922731	0.70533544547537	2.37e−008

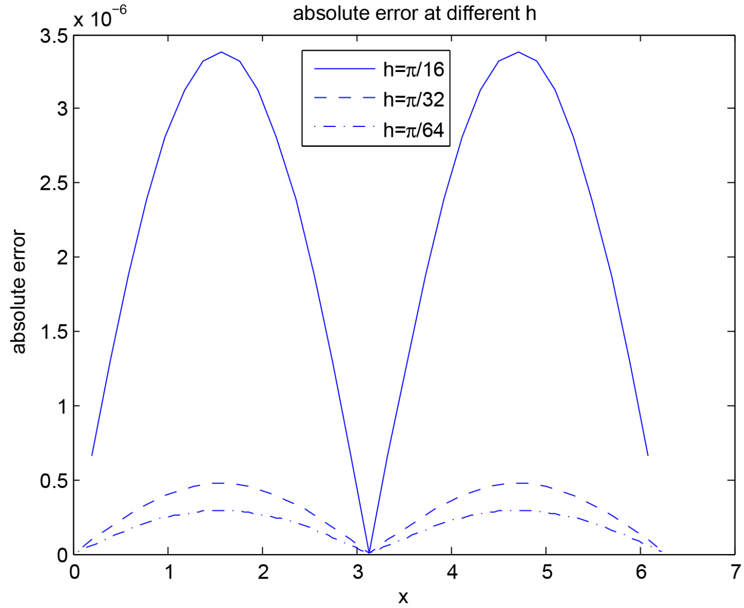

Figure 1. The absolute error at different h for example 1 with $k = 0.001, t = 1$.

Table 3. Conserved quantities and error norms at various times for example 2 with $k = 0.01, h = 0.1, a = -10, b = 20$.

t	C_1	C_2	L_∞	L_2	E^r
1	1.25331413731550	−3.31870453365852	2.1940e-003	2.8448e-003	2.5411e-003
2	1.25331413731550	−3.33237042327679	2.3980e-004	3.2407e-003	2.8948e-003
3	1.25331413731550	−3.32685242595849	7.7694e-004	9.4702e-004	8.4592e-004
4	1.25331435202165	−3.31733074605112	2.2382e-003	2.5906e-003	2.3140e-003

$C_1^{0exact} = C_1^0 = 1.25331413731550, C_2^{0exact} = C_2^0 = -3.32358067657703$

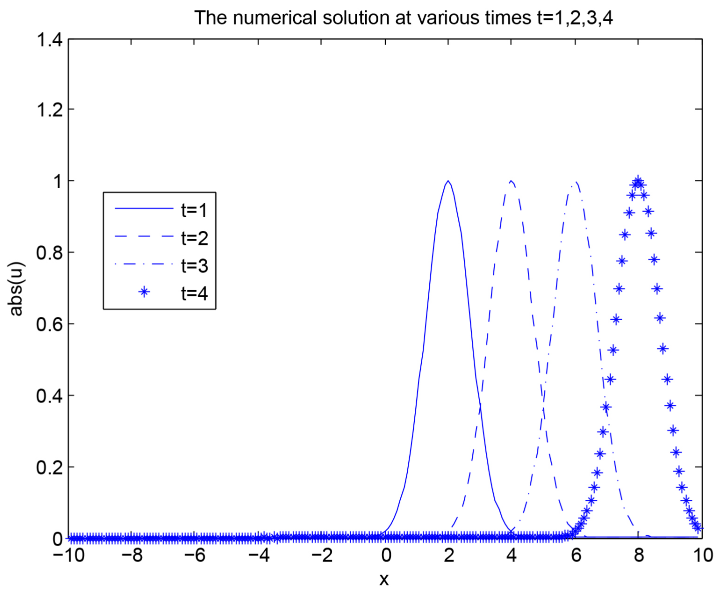

Figure 2. The numerical solution at various times t = 1, 2, 3, 4 with $k = 0.01, h = 0.1$.

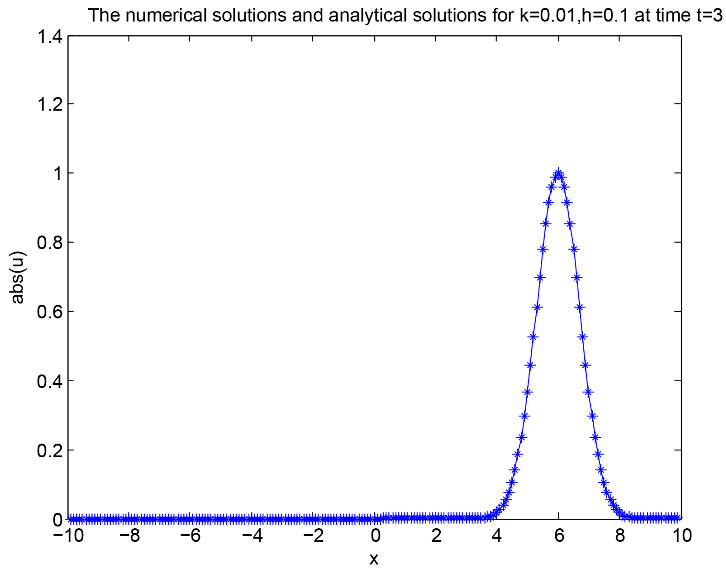

Figure 3. The numerical solutions and analytical solutions for $k = 0.01$, $h = 0.1$ at time $t = 3$.

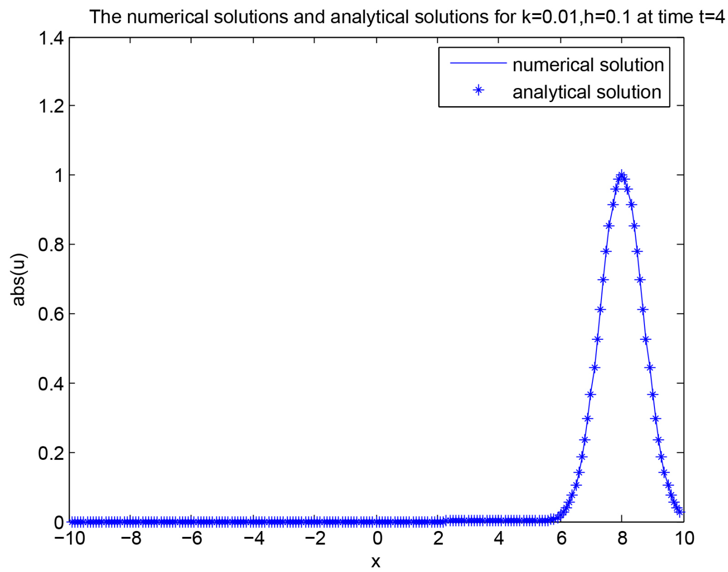

Figure 4 The numerical solutions and analytical solutions for $k = 0.01$, $h = 0.1$ at time $t = 4$.

Conserved quantities and error norms at various times are presented in **Table 3**. The numerical results reveal that the values of C_1 is almost constant while the values of C_2 differ slightly and the errors are very small.

The numerical solutions at various times are given in **Figure 2**. The numerical solutions and analytical solutions at time $t = 3$ and $t = 4$ are shown in **Figure 3** and **Figure 4**, respectively. The absolute error at time $t = 3$ and $t = 4$ are plotted in **Figure 5** and **Figure 6**, respectively. It observed that (1) the propagation of solitary wave is rightward while preserving unchanged shape; (2) our method gives a good approximation compared with the exact solutions.

6. Conclusion

A numerical method based on exponential spline interpolation function is applied to study a class of nonlinear Schrödinger equation. We use exponential spline collocation method, which results in tri-diagonal systems of

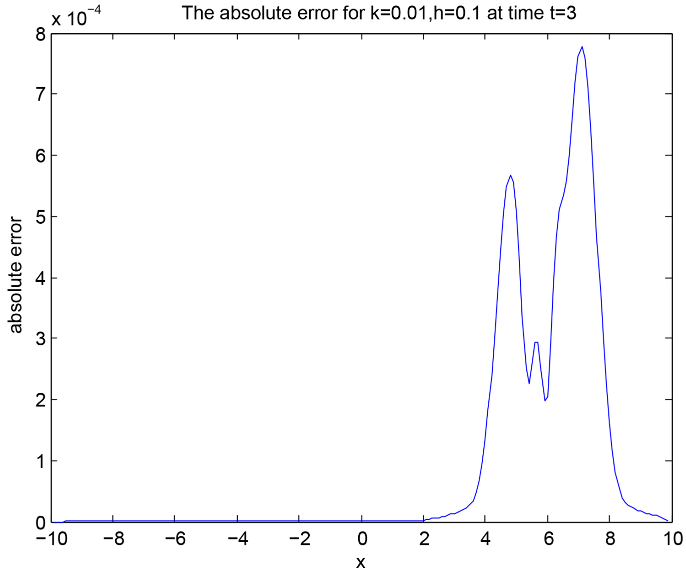

Figure 5. The absolute error for $k = 0.01$, $h = 0.1$ at time $t = 3$.

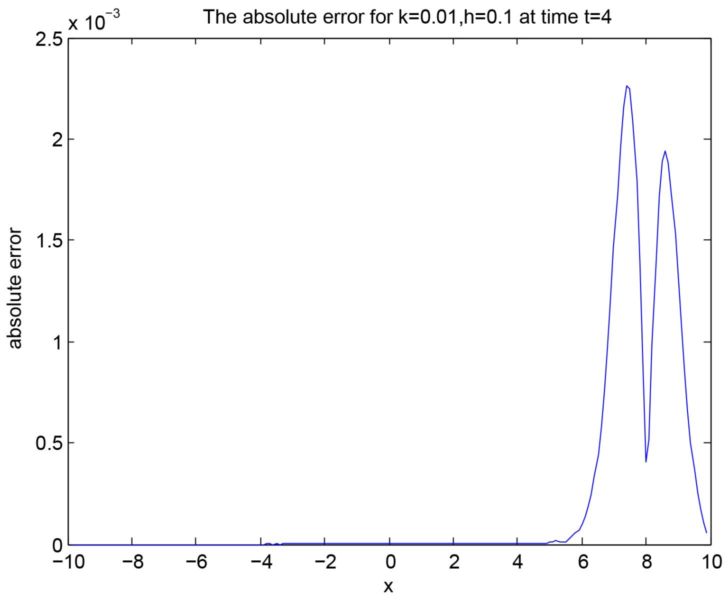

Figure 6. The absolute error for $k = 0.01$, $h = 0.1$ at time $t = 4$.

equations that can be solved efficiently by the Thomas algorithm. The numerical simulations confirm and demonstrate the reliability and efficiency of the schemes and tell us that the method is applicable technique, relatively simple and approximates the exact solution very well.

Acknowledgements

The authors would like to thank the editor and the reviewers for their valuable comments. This work was supported by the Natural Science Foundation of Guangdong (2015A030313827).

References

[1] Infeld, E. (1984) Nonlinear Waves: From Hydrodynamics to Plasma Theory, Advances in Nonlinear Waves. Pitman, Boston.

[2] Nore, C., Abid, A. and Brachet, M. (1996) Small-Scale Structures in Three-Dimensional Hydrodynamics and Magnetohyrodynamic Turbulence. Springer, Berlin.

[3] Agrawal, G.P. (2001) Nonlinear Fibei Optics. 3rd Edition, Academic Press, San Diego.

[4] Fordy, A.P. (1990) Soliton Theory: A Survey of Results. Manchester University Press, Manchester.

[5] Bruneau, C.H., Di Menza, L. and Lerhner, T. (1999) Numerical Resolution of Some Nonlinear Schrödinger-Like Equation in Plasmas. *Numerical Methods for Partial Differential Equations*, **15**, 672-696. http://dx.doi.org/10.1002/(SICI)1098-2426(199911)15:6<672::AID-NUM5>3.0.CO;2-J

[6] Bang, O., Christiansen, P.L., Rasmussen, K. and Gaididei, Y.B. (1995) The Role of Nonlinearity in Modeling Energy Transfer in Schibe Aggregates. In: *Nonlinear Excitations in Biomolecules*, Springer, Berlin, 317-336. http://dx.doi.org/10.1007/978-3-662-08994-1_24

[7] Ferreira, M.F., Faco, M.V., Latas, S.V. and Sousa, M.H. (2005) Optical Solitons in Fibers for Communication Systems. *Fiber and Integrated Optics*, **24**, 287-313. http://dx.doi.org/10.1080/01468030590923019

[8] Zhang, J.F., Dai, C.Q., Yang, Q. and Zhu, J.M. (2005) Variable-Coefficient F-Expansion Method and Its Application to Nonlinear Schrödinger Equation. *Optics Communications*, **252**, 408-421. http://dx.doi.org/10.1016/j.optcom.2005.04.043

[9] Zhang, J.L., Li, B.A. and Wang, M.L. (2009) Soliton Propagation in a System with Variable Coefficients. *Chaos Solitons Fractals*, **39**, 858-865. http://dx.doi.org/10.1016/j.chaos.2007.01.116

[10] Taha, T.R. and Ablowitz, M.J. (1984) Analytical and Numerical Aspects of Certain Nonlinear Evolution Equations. II. Numerical, Nonlinear Schrödinger Equation. *Journal of Computational Physics*, **55**, 203-230. http://dx.doi.org/10.1016/0021-9991(84)90003-2

[11] Zhang, L. (2005) A High Accurate and Conservative Finite Difference Scheme for Nonlinear Schrödinger Equation. *Acta Mathematicae Applicatae Sinica*, **28**, 178-186.

[12] Duan, A. and Rong, F. (2013) A Numerical Scheme for Nonlinear Schrödinger Equation by MQ Quasi-Interpolatin. *Engineering Analysis with Boundary Elements*, **37**, 89-94. http://dx.doi.org/10.1016/j.enganabound.2012.08.006

[13] Dag, I. (1999) A Quadratic B-Spline Finite Element Method for Solving Nonlinear Schrödinger Equation. *Computer Methods in Applied Mechanics and Engineering*, **174**, 247-258. http://dx.doi.org/10.1016/S0045-7825(98)00257-6

[14] Dehghan, M. and Taleei, A. (2010) A Compact Split-Step Finite Difference Method for Solving the Nonlinear Schrödinger Equations with Constant and Variable Coefficients. *Computer Physics Communications*, **181**, 43-51. http://dx.doi.org/10.1016/j.cpc.2009.08.015

[15] Dehghan, M. and Taleei, A. (2011) A Chebyshev Pseudospectral Multidomain Method for the Soliton Solution of Coupled Nonlinear Schrödinger Equations. *Computer Physics Communications*, **182**, 2519-2529. http://dx.doi.org/10.1016/j.cpc.2011.07.009

[16] Mohammadi, R. (2014) An Exponential Spline Solution of Nonlinear Schrödinger Equations with Constant and Variable Coefficients. *Computer Physics Communications*, **185**, 917-932. http://dx.doi.org/10.1016/j.cpc.2013.12.015

[17] Lin, B. (2013) Parametric Cubic Spline Method for the Solution of the Nonlinear Schrödinger Equation. *Computer Physics Communications*, **184**, 60-65. http://dx.doi.org/10.1016/j.cpc.2012.08.010

[18] Lin, B. (2015) Septic Spline Function Method for the Solution of the Nonlinear Schrödinger Equation. *Applicable Analysis*, **94**, 279-293. http://dx.doi.org/10.1080/00036811.2014.890709

[19] Wang, S.S. and Zhang, L. (2011) Split-Step Orthogonal Spline Collocation Methods for Nonlinear Schrödinger Equations in One, Two, and Three Dimensions. *Applied Mathematics and Computation*, **218**, 1903-1916. http://dx.doi.org/10.1016/j.amc.2011.07.002

[20] Mohebbi, A. and Dehghan, M. (2009) The Use of Compact Boundary Value Method for the Solution of Two-Dimensional Schrödinger Equation. *Journal of Computational and Applied Mathematics*, **225**, 124-134. http://dx.doi.org/10.1016/j.cam.2008.07.008

[21] Ismail, M.S. and Taha, T.R. (2007) A Linearly Implicit Conservative Scheme for the Coupled Nonlinear Schrodinger Equation. *Mathematics and Computers in Simulation*, **74**, 302-311. http://dx.doi.org/10.1016/j.matcom.2006.10.020